http://journal.uir.ac.id/index.php/JGEET

E-ISSN : 2541-5794
P-ISSN : 2503-216X

Journal of Geoscience,
Engineering, Environment, and Technology
Vol 11 No 1 2026

RESEARCH ARTICLE

Soft Layer Identification In Kedamaian District Using the HVSR-Derived Shear Wave Velocity Distribution

Galang Dwi Mulyana[1], Risky Martin Antosia[2*], Edlyn Yoadan Nathania[3]
[1, 2, 3] *Department of Geophysical Engineering, Faculty of Industrial Technology, Institut Teknologi Sumatera, Lampung, Indonesia.*

* Corresponding author : martin.antosia@tg.itera.ac.id
Tel.:+62 813 20353544
Received: Oct 23, 2025; Accepted: Mar 13, 2026.
DOI: 10.25299/jgeet.2026.11.1.25294

Abstract

The Kedamaian District in Bandar Lampung City is a densely populated urban area characterized by complex geological settings that are highly susceptible to seismic amplification and geotechnical hazards. Despite its vulnerability, high-resolution characterization of subsurface soft soil deposits in this specific district remains underexplored. The study aims to evaluate local site effects for designing seismic-resistant infrastructures and mitigating geotechnical hazards. This study attempts to locate and determine the characteristics of soft soil deposits in the Kedamaian District, Bandar Lampung City, by means of the HVSR method (Horizontal to Vertical Spectral Ratio) based on the shear wave velocity distribution result. Microtremor measurements were taken from 37 points and processed to estimate the amplification factor (A_0), dominant frequency of soil deposit (f_0), and seismic vulnerability index (K_g). HVSR inversion used the Particle Swarm Optimization (PSO) to propose average shear wave velocity down to 30 m depth (V_S^{30}). Analysis indicated that the amplification values range from 2.31 to 9.11, with most values falling within a moderate level, indicating a moderate local site response. Dominant frequencies range from 0.63 to 18.76 Hz, and higher f_0 values are characteristic of more compact and/or complex rock formations, whilst lower f_0 values correspond to thicker sediments. Values of the seismic vulnerability index range from 0.48 to 119.24 s, with most sites showing a high seismic vulnerability related to the combined effect of high amplification and low dominant frequency. The distribution suggests that the study region consists predominantly of soft soils (type E) with V_S^{30} ranging from 80.9 to 132.6 m/s, interspersed with medium soils (type D) and less abundant hard rocks (type C). The results show that the Kedamaian is primarily covered with soft sediment formations, which have the potential to enhance strong ground motion during seismic events, as well as for a geotechnical investigation database and hazard assessment of earthquake activities and urban development within the region.

Keywords: HVSR method, shear wave velocity, seismic vulnerability, microtremor, Kedamaian District, Particle Swarm Optimization

1. Introduction

The Kedamaian District in Bandar Lampung City features a moderately flat topography with gentle hills, reflecting geological complexity in the shallow sediment layers. The surrounding area has developed rapidly, characterized by high population density and strong demand for land and infrastructure. These environments require a thorough understanding of the properties of the shallow sediments to support their sustainable development. The geological setting of Kedamaian contributes to soil instability, making the area susceptible to geological hazards such as liquefaction, land subsidence, and earthquake amplification waves. Local factors, such as soil conditions, significantly contribute to the extent of damage caused by an earthquake (Işık et al., 2025; Simanjuntak et al., 2025; Yatini et al., 2023), so infrastructure must be carefully assessed to mitigate the effects of earthquakes.

The Horizontal to Vertical Spectral Ratio (HVSR) method is a useful geophysical technique for mapping shallow sediments, as it enables the determination of the dominant frequency, amplification, and thickness of sediment without causing any noticeable environmental impact. The core of HVSR is to discover the resonance frequency of the soil, and it depends on the thickness and stiffness of each layer (Amirudin et al., 2023; Apriana et al., 2025; Khayati et al., 2022; Ma and Liao, 2024; Manan et al., 2023; Simanjuntak et al., 2025; Yatini et al., 2023). As a widely applied inversion technique of geophysical modelling and signal analysis, Particle Swarm Optimization (PSO) is utilized to search for model parameters which provide the best fit to observational data. This method emulates the collection of particles traversing a solution space, with each particle updating its position and velocity based on its individual experience and the experiences of other particles in the group (Yudha et al., 2023). PSO is an expressional etiquette among those population-based algorithms which could be used in multidisciplinary domains. In artificial intelligence, it has served a great part for neural network training and feature selection (Mahapatra et al., 2023). The use of PSO has further spread to the medical field such as medical image segmentation (MRI, CT scans) (Kubicek et al., 2023) and optimal dose planning in radiotherapy (Künzel et al., 2020).

The research by Zaenudin et al. (2022), who estimated shear wave velocity (V_S) in Bakauheni, South Lampung, with an inversion process of the HVS ratio that was optimized by the PSO method. Microtremor measurements were taken at seven recording stations and analyzed to obtain HVSR curves, which were then jointly inverted using PSO. The results obtained are compared with those of the Genetic Algorithm (GA). Synthetic experiments demonstrated that the convergence rate, stability, and noise insensitivity of PSO were superior to those of GA. By using the field data, they could create a 2D model that showcased sedimentary layers with basement, and also one that verified the presence of the Way Baka Fault as indicated by paleoseismic studies. The PSO-based HVSR method has been proven to be a viable approach for mapping geologic features without prior data. It has good applicability for mitigating geological hazards in earthquake-prone areas.

However, earlier research in the Lampung region has tended to concentrate on areas of the southern coastal zones, such as Bakauheni, or highland/hilly areas on the border of the Bandar Lampung area, such as the Kemiling area (Ariyanto et al., 2024). In contrast, little is known about the Kedamaian District, despite its high population density (Nasrudin et al., 2024), where seismic amplification is likely to occur. In addition, few established works have coupled HVSR data inversion with PSO techniques to characterize the shear wave velocity distribution at acceptable spatial resolution in urban environments. Filling this knowledge gap is crucial for local site characterization and determining site-specific parameters for seismic hazard mitigation.

Accordingly, this research aims to determine and characterize the soft soil layer in the Kedamaian District region by employing the HVSR method that is constructed from shear wave velocity distribution. The findings are also anticipated to be valuable reference data for the design of seismic-resistant constructions, as well as to enhance the engineering geology databank in support of urban development planning purposes in Bandar Lampung.

2. Methodology

2.1 Regional Settings

The location of Lampung Province is generally in the Barisan Zone (Hilly Region). This zone is approximately 1,650 km long and about 100 km wide, characterized by a long, narrow strip that extends in the figure from southeast to northwest. The area represents a seismically active region due to the interplay between the Eurasian and Indo-Australian plates with complex lithological and structural heterogeneity.

The stratigraphic sequence of the Kedamaian District consists of Quaternary and Tertiary rocks. The Quaternary deposits (Pleistocene-Holocene) are dominated by volcanic materials, which consist of the Young Volcanic Deposits (Qh) and the Lampung Formation (Qt1), represented by pumice tuff, tuffaceous clay, and sandstone. These masses were created by successive eruptions of volcanoes, which produced massive pyroclastic and reworked volcanic deposits.

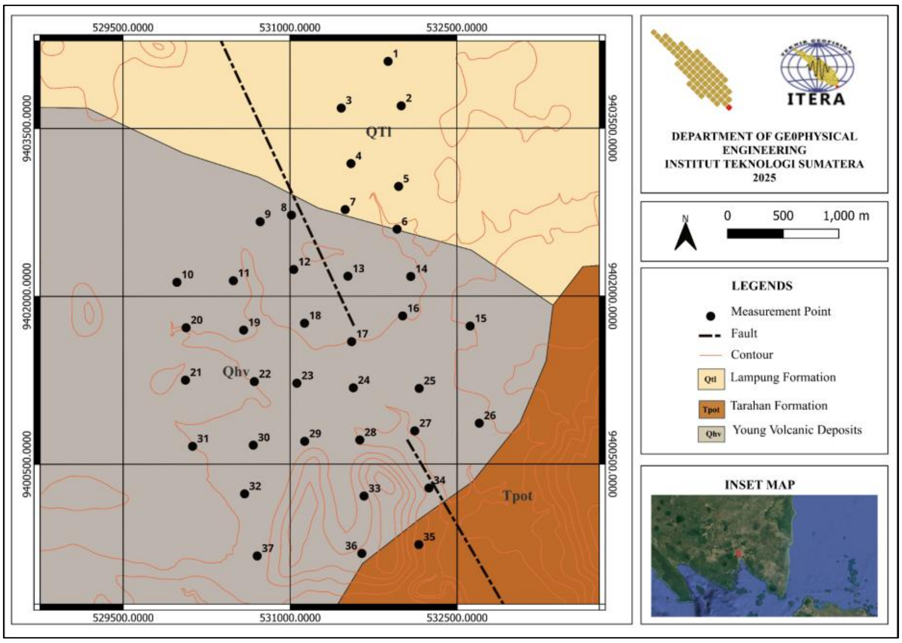

Fig. 1. Regional geological map of the study area (modified from Mangga et al., 2010)

The Tertiary sequence underlies them and consists of Sabu Formation (Tpos), Campang Formation (Tpoc), and Tarahan Formation (Tpot), which were deposited during Paleocene to Oligocene. The Sabu Formation is unconformably overlying the Pre-Tertiary basement and underlain by the Hulusimpang Formation (Tomh), Late Oligocene to Early Miocene, indicating tectonic uplift and regional deformation. Later in the Miocene, sedimentation environments changed from deep marine to shallow marine and estuarine, to form the Kantur (Tmpk) and Surungbatang (Tmps) Formations during the Early Pliocene. The Barisan Arc tectonovolcanism and the down-dip subduction to the southwest are later responsible for generating the andesitic lavas, which are one of the most well-recognized characteristics in the regional geology (Mangga et al., 2010).

As shown in Fig. 1, the study area is composed of three core geological formations: Lampung Formation (Qtl), Tarahan Formation (Tpot), and Young Volcanic Deposits (Qhv). The Lampung Formations are dominated by volcanic rocks, such as pumice tuff, rhyolitic tuff, welded tuff, tuffite, tuffaceous clay, and lithic sandstone, suggesting the condition of intensive volcanism during the Lampung Formation's deposition. The Tarahan Formation consists of mineralized volcanic rocks, mainly welded tuff and layered chert breccia, and tuffaceous breccia with clasts of andesitic–basaltic lava indicating a proximal volcanic provenance. The stratigraphic relationships of this formation are correlated with the Sabu and Campang Formations, implying a genetic correlation between these volcanic-sedimentary formations. In addition, the Young Volcanic Deposits (Qhv), composed of andesitic–

basaltic lava, volcanic breccia, and Holocene tuff, suggest that activity may have continued into the present time.

2.2 HVSR Method

The Horizontal to Vertical Spectral Ratio (HVSR) technique is a fast, non-invasive, inexpensive microtremor survey applicable in residential and urban areas. It applies three-component seismic records for studying local site effects and microzonation. The technique was originally proposed by Nogoshi and Igarashi (Molnar et al., 2018) and further developed by Nakamura (Nakamura, 2019). Microtremors, which are the foundation for this approach, refer to low-amplitude ground vibrations caused by either natural or human-induced sources such as ocean waves, winds, traffic, and industrial facilities (Antsiferov et al., 2025). These vibrations, usually in the frequency range 0.05–100 Hz, include information about surface descriptors of underground resonance properties. The HVSR method is based on comparing Fourier's amplitude spectra of the horizontal (north–south and east–west) and vertical components to allow for estimating the natural frequency and amplification factor of the soil (Eqn. (1)). In the study area, 37 sites were measured by HVSR in this survey (Fig. 1).

$$HVSR = \frac{\sqrt{(S_{NS})^2 + (S_{EW})^2}}{S_V} \quad (1)$$

S_{NS} and S_{EW} are the spectral amplitudes of the north-south and east-west components, respectively. S_V is the spectral amplitude of the vertical component.

The natural frequency (f_0) is the basic resonance of the soil layer and depends on shear wave velocity (V_S) and sediment height. A lower natural frequency is obtained with increased sediment depth. The depth of the sediments on top of the rock. It is critical for the interpretation of subsurface geological structures because it represents the rigidity and depth of sedimentary strata. A highly dominant frequency is usually related to stiff or dense formation and thin sediment. In contrast, a low dominant frequency is indicative of thick and unconsolidated files that are effective in the amplification of seismic waves. This is the frequency which corresponds to the maximum of H/V (Saadalla et al., 2023). The soil classification for natural frequency values is given in Table 1.

Table 1. Soil classification based on natural frequency from Kanai (Ariyanto et al., 2024).

Type	f_0 (Hz)	Description
I (Hard soil)	6.67 – 20	Thin sediment layer dominated by hard rock.
II (Medium soil)	4 – 6.67	Alluvial deposits (~5–10 m) of sandy clay and gravel.
III (Thick soil)	2.5 – 4	Alluvial deposits (~10–30 m) of sandy clay and loam.
IV (Very thick soil)	<2.5	Deltaic or muddy alluvium with high sediment thickness.

Amplification (A_0) represents the wave amplitude amplification caused by the impedance contrast between soft and hard layers. Amplification of seismic waves through layers with contrasting physical properties increases the ground motion (Nateqi et al., 2025; Wang et al., 2024). Such a setting is often encountered when waves go from firm bedrock into more plastic, thicker sedimentary deposits (Nateqi et al., 2025). The change in velocity of waves allows the seismic energy to get inside and be trapped into the pores of the sediment – enhanced ground vibrations at the surface. Table 2 overviews the different amplification levels.

The seismic vulnerability index (K_g), first proposed by Nakamura (Nakamura, 2019), is expressed by:

$$K_g = \frac{(A_0)^2}{f_0} \quad (2)$$

Higher K_g values indicate that the sediments are thicker and more susceptible to damage from earthquakes. Table 3 shows how K_g values are grouped.

Table 2. Classification of amplification factor values (Apriana et al., 2025; Ariyanto et al., 2024).

Type	Amplification (A_0)	Classification
I	$A_0 < 3$	Low
II	$3 \le A_0 < 6$	Moderate
III	$6 \le A_0 < 9$	High
IV	$A_0 \ge 9$	Very high

Table 3. Grading of seismic vulnerability index values (Ariyanto et al., 2024).

Type	K_g (s)	Description
I	K_g <3	Low
II	3≤ K_g <6	Moderate
III	K_g >6	High

2.3 Shear Wave Velocity (V_S)

The shear-wave (S-wave) velocity is an important intrinsic material property that represents the stiffness and elastic behavior of subsurface lithologies, therefore directly affecting the site amplification factor. The parameter V_S^{30} is taken as the mean shear-wave velocity of the upper 30 m of soil (Eq. (3)) and is considered a good measure of the soil's strength and dynamic performance (Ahadi et al., 2023; Xv and Li, 2023). For geotechnical and seismic purposes, V_S^{30} is a well-known measure of the classification of a site or for engineering design works because it relates to how well the near-surface material can transmit, amplify, or attenuate the propagated seismic waves. Lower V_S^{30} values indicate weak or small-based soft sediments with larger amplification when it occurs, while higher values mean relatively strong or loose ones and distributions that tend to damp the seismic energy.

$$V_S^{30} = \frac{30}{\Sigma\left(\frac{h_i}{V_{Si}}\right)} \quad (3)$$

where h_i is the thickness of layer i and V_{S_i} its shear wave velocity. Table 4 shows that the V_S^{30} classification.

Table 4. Soil classification based on V_S^{30} based on SNI 1726:2019 (Wibowo et al., 2024).

Type	Classification	V_S^{30} (m/s)
A	Hard rock	>1500
B	Rock	750-1,500
C	Hard to medium soil and soft rock	350-750
D	Medium soil	175-350
E	Soft soil	<175

2.4 Particle Swarm Optimization (PSO) Inversion

The HVSR curves are inverted, and shear wave velocity profiles are estimated using the Particle Swarm Optimization (PSO) algorithm. PSO is one of the optimization algorithms that processes a population of particles iteratively to search for a solution space by adjusting the velocity and position in plotting each particle influenced by the personal best obtained and the global best experienced value (Farduwin et al., 2021; Farduwin and Yudistira, 2021; Yudha et al., 2023). The update equations are given by:

$$V_i^{t+1} = \omega V_i^t + c_1 r_1 \left(P_{best(i)} - P_i^t\right) + c_2 r_2 \left(G_{best} - P_i^t\right) \quad (4)$$

$$P_i^{t+1} = P_i^t + V_i^{t+1} \quad (5)$$

where V_i is the velocity, P_i is the position of the particle, ω is the inertia weight, $c_1$and c_2 are acceleration coefficients, and r_1, r_2 are random numbers between 0 and 1. Calibrating the population size, inertia weight, and acceleration parameter correctly ensures that the algorithm converges on the best solution.

3. Results and Discussion

Table 5-HVSR data processing results, including A_0 and f_0 values at each measuring point and the relevant seismic vulnerability index (K_g), which was calculated based on Eqn. (2). These quantities are key drivers of the shallow subsurface dynamics for the domain under investigation. Heterogeneity in A_0 and f_0 patterns indicates sediment thickness and stiffness contrasts, whereas K_g indicates increasing/decreasing seismic vulnerability among the surveyed sites.

Table 5. Amplification value, dominant frequency, and seismic vulnerability index.

Point	A_0	f_0 (Hz)	K_g (s)	Point	A_0	f_0 (Hz)	K_g (s)
T1	2.45	12.06	0.50	T20	5.96	0.68	52.39
T2	5.44	0.65	45.77	T21	6.64	0.67	65.41
T3	7.20	0.64	80.94	T22	5.96	0.69	51.06
T4	8.76	0.67	115.42	T23	6.27	0.65	60.31
T5	4.34	0.68	27.57	T24	8.51	0.65	111.76
T6	3.72	3.98	3.47	T25	6.64	0.74	59.36
T7	3.51	2.03	6.07	T26	2.71	0.71	10.35
T8	4.37	1.59	12.03	T27	3.86	0.71	20.94
T9	4.60	0.65	32.50	T28	4.45	9.57	2.07
T10	6.38	0.67	60.54	T29	3.45	0.84	14.26
T11	9.11	0.70	119.24	T30	4.69	0.66	33.30
T12	3.56	18.11	0.70	T31	6.44	18.01	2.30
T13	5.86	2.08	16.47	T32	2.52	8.53	0.75
T14	5.59	11.49	2.72	T33	5.09	0.67	38.42
T15	3.99	12.47	1.28	T34	8.40	0.63	112.86
T16	4.25	2.04	8.87	T35	5.39	18.76	1.55
T17	6.05	0.64	57.34	T36	5.78	0.64	52.37
T18	3.89	3.64	4.15	T37	7.24	10.17	5.15
T19	2.31	11.04	0.48				

3.1 Distribution of Amplification Factor Values

Table 5 shows that the amplification values fall within the range of 2.31 to 9.11, based on the processing results. The maximum value of amplification is observed at the T11 point, and the minimum value is observed at the T19 point. Low amplification rates are found at T1, T26, T19, and T32 points; and most parts of the studied area remain at a moderate level of 3.51 to 5.78. Values of seismic amplification in many places are observed to be high (7.20–8.76) and very high amplification at a place like T11, respectively.

As shown in Table 6, the study area is mainly dominated by modest amplification types, which means that although local ground motion is noticeable, it would not exceed a moderate level of origin hazard. As illustrated in Fig. 2, the curve of amplification values throughout the study area follows the geological traits of each formation. Within the Lampung Formation, in T3 and T4, relatively high amplification is encountered, while mostly moderate values are found in those areas covered by T2, T5, T6, and T7. This behavior corresponds with the lithological composition of compact tuff, rhyolitic tuff, tuffite, tuffaceous clay, and tuffaceous sand. The cross-impedance contrast of these media is moderate, corresponding to medium amplification.

In the Quaternary Volcanic Deposits, amplification ranges from low to high, and very high values are present in some areas. The greatest amplification is at T11, which means that there are thick and loosely consolidated volcanic products in the area with a strong seismic wave amplifying effect. The Tarahan Formation, on the other hand, exhibits generally moderate to low amplification with point T35 as a representative point, suggesting moderately consolidated volcanic and sedimentary rocks. This formation consists mainly of breccia interbedded with chert, tuff, and tuffaceous breccia and reflects modest sediment thickness and a moderate seismic response.

Table 6. Classification of amplification factor values in the study area.

Point	Type
T1, T26, 219, T32	Low
T2, T5-T19, T12-T16, T18, T20, T22, T27-T30, T33, T35-T36	Moderate
T3-T4, T10, T17, T21, T23-T25, T311, T34, T37	High
T11	Very high

The response to earthquakes of soils as a medium for the propagation of waves is also affected by their mechanical properties. According to Fitriana et al. (2019), hard ground typically has low attenuation, which means that seismic waves can travel with little energy loss, whereas soft sediment shows high attenuation and results in stronger surface waves due to the trapping and scattering of energy within the sediment. That's why the regions featuring soft sediments at T11 have a higher value of amplification. On the other hand, areas with compact or cemented deposits receive smaller amplification, since seismic energy is absorbed faster in denser media.

These results indicate that the area of Kedamaian poses a relatively low risk to suffer structural damage due to an earthquake since the majority of zones have small to moderate amplification factors.

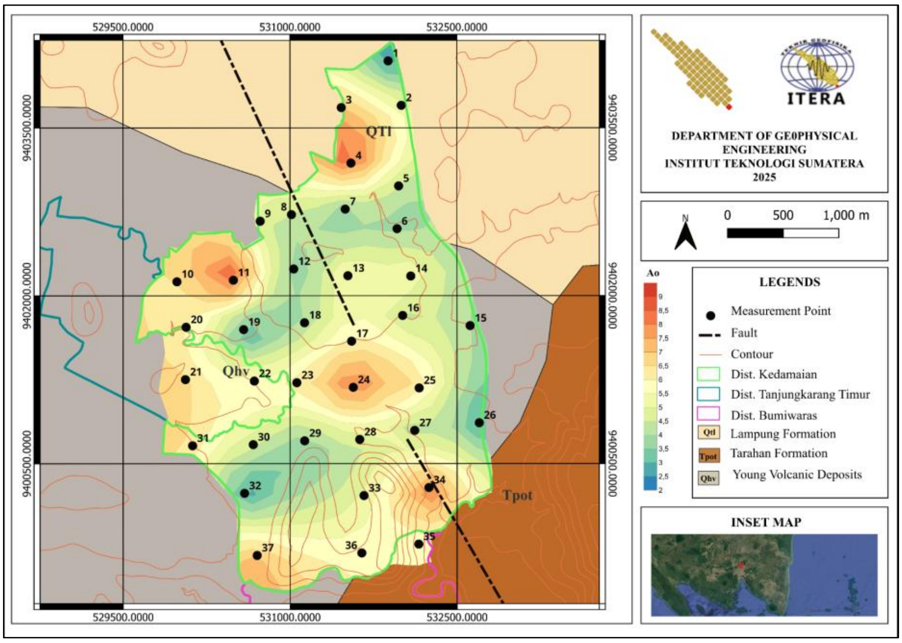

Fig. 2. Amplification distribution map of the study area overlaid with geological formations.

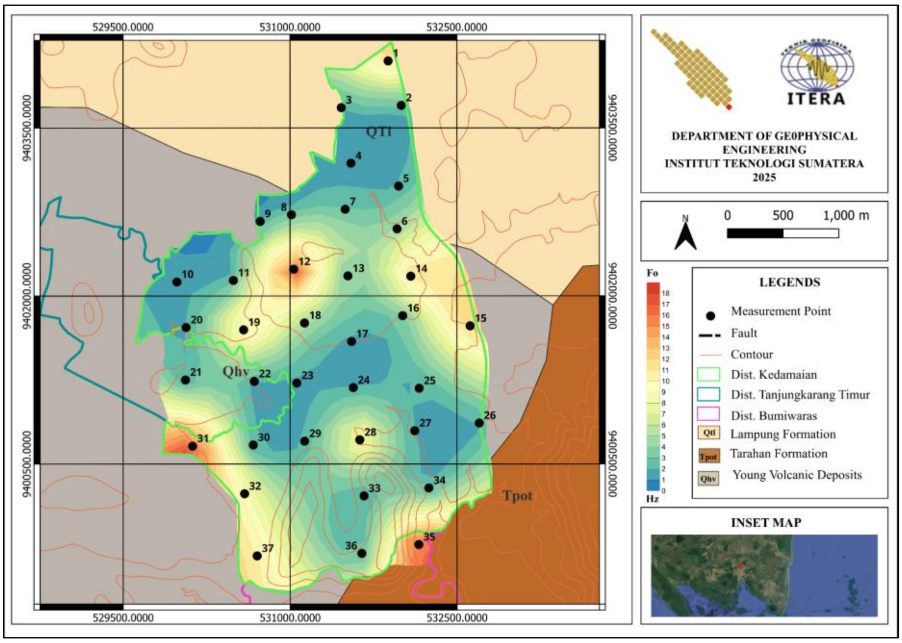

Fig. 3. Geological features overlaid on the dominant frequency distribution map of the study region.

3.2 Distribution of Dominant Frequency Values

As shown in Table 5, the value of dominant frequency with respect to the Kedamaian district varies from 0.63 Hz to 18.76 Hz, with significant spatial variation evident. Ten measurement points are of type I, showing high dominant frequency values, corresponding to regions dominated by hard rock with very thin sediment cover. The other two points belong to type II (zones with an average thickness from 5 to 10 meters of sedimentary cover), and the most, 25 points, are classified as type IV (very thick sedimentary covers). These categories are shown in Table 7.

Table 7. Classification of dominant frequency.

Point	Type
T1, T12, T14-T15, T19, T28, T31-T32, T35, T37	I
T6, T18	II
T2-T5, T7-T11, T13, T16-T17, T20-T27, T29-T30, T33-T34, T36	IV

As illustrated in Fig. 3, spatial variations of f_0 are clearly consistent with geological structures in the study area. Based on classification by Kanai (Ariyanto et al., 2024), the Lampung Formation is mainly characterized by low-frequency (type IV) values between 0.63 and 2.08 Hz, which implies thick sediment fill with tuffaceous and volcanic sediments dominating the deposit. The Young Volcanic Deposits, however, exhibit a broader frequency range—lower to higher frequencies—and a more complex base of valley tuning. Ten measurement points of those considered here, some fall in type I (8.53–18.76 Hz), indicating shallow bedrock and compact volcanic rocks; others belong to type II (3.64–3.98 Hz) meaning moderately thick sediments are present in the area.

This variation mainly results from different levels of sediment consolidation, varying lithology, and local structural setting. Low dominant frequencies are expected in areas of high sediment thickness with low shear-wave velocities and possible resonance conditions for long-period ground motion. On the other hand, high-dominant-frequency zones are commonly associated with compact volcanic or basement units, possibly capable of attenuating seismic energy more efficiently and less prone to resonance amplification.

The correlation of these amplification factors (A_0) and the distribution means a reciprocal relation; locations with low f_0 are associated consecutively with relatively higher amplifications. This correlation corroborates the interpretation that softer and thicker sediments amplify more effectively seismic waves because they trap and scatter seismic energy. As noted by Yao and Wu (2024), the soft soil sediments have strong attenuation, where wave energy is absorbed and re-radiated in a layer, resulting in long shaking. Inversely, stiff soils and those with low attenuation permit passage of seismic waves through large distances for minimum energy dissipation, hence a site has a higher dominant frequency but lower amplification.

As an overall, spatial pattern of dominant frequency across the Kedamaian District shows that most of the investigation area dominated by thick and soft site, especially in the part of Lampung Formation. This implies that site effects are more sensitive, and resonance phenomena could develop during intense shaking.

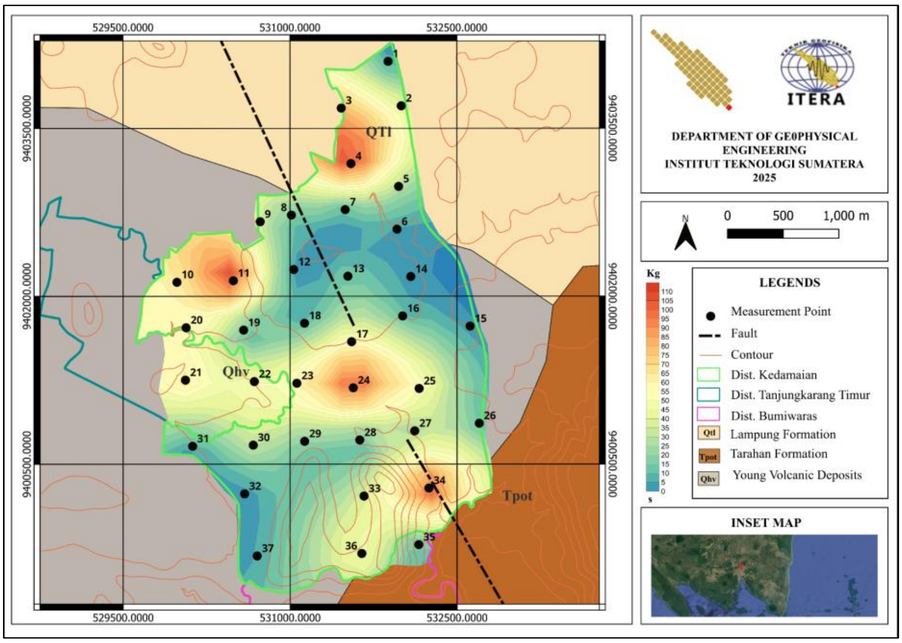

Fig. 4. Seismic vulnerability index distribution map of the study area overlaid with geological formations.

3.3 Distribution of Seismic Vulnerability Index Values

Results presented in Table 5 show that the seismic vulnerability index ranges between 0.48 and 119.24 in the Kedamaian area; this high variability reflects heterogeneous soil properties beneath the region. According to the classification thresholds proposed in this investigation, nine measurements are of low vulnerability (0.48-2.72), three of moderate (3.47-5.15), and twenty-five are high vulnerability (6.07-119.24). This large range indicates that seismic motions in the study region are greatly affected by local geological conditions. The categorizations are observed in Table 8.

As illustrated in Fig. 4, the Lampung Formation consists mostly of high K_g values indicative of thick, unconsolidated sediment with a low A_0 and high f_0. Such geological site effects increase acceleration amplification factors and duration of ground shaking, thus exposing more vulnerability against strong shaking. However, certain points, e.g., T1 have low K_g, which means that the lithology of the ground is dense and shallow depth due to bedrock, where the rate of ground amplification factor is significantly reduced.

The Young Volcanic Deposits Formation exhibits moderate to high K_g values, which are indicative of its heterogeneity in terms of lithology. The heterogeneous distribution of K_g with this formation implies alternating bands of dense vesicular volcanic rocks and unconsolidated pyroclastic deposits, leading to localized resonant effects.

Spatially, higher values tend to be localized in southern and central Kedamaian with the thickest sedimentary deposits of the Lampung Formation. These zones display high impedance contrasts between the soft surface layers and stiff bedrock below, which can capture and focus seismic waves. This is consistent with the result of dominant frequency (Section 3.2), i.e., low f_0 with higher K_g values.

Table 8. Results of seismic vulnerability index values.

Point	Type
T1, T12, T14-T15, T19, T28, T31-32, T35	Low
T6, T18, T37	Moderate
T2-T5, T7-T11, T113, T16, T17, T20-T27, T29-T30, T33-T34, T36	High

The relationship between A_0, f_0, and K_g highlights the importance of both the sediment thickness and stiffness contrast in governing local seismic responses. As observed by Nakamura (Nakamura, 2019) and later works (e.g. Amirudin et al., 2023; Asnawi et al., 2023; Dewi et al., 2023; Prasetya et al., 2024; Risa et al., 2023), sites with a higher K_g tend to have higher ground shaking amplification and correspondingly higher potential for damage, particularly for low-rise buildings with natural frequencies close to that band. Accordingly, the high K_g zones detected by this study need to be taken into account in urban development, seismic microzonation, and earthquake-resistant design.

Overall, the geospatially distributed values over the Kedamaian are in a high-vulnerable region, with a majority of the study area being covered by medium to thick unconsolidated sediments that have a strong potential for significant ground motion amplification.

3.4 Inversion Processing Results

Fig. 5 shows the inversion results of the model at the Kedamaian area, depicting vertical and lateral variation of soil stiffness. The approach model used in the inversion is a five-layer one, which adopts a similar methodology to that of Zaenudin et al. (2022), who used the same technique in Bakauheni with a similar geological structure. The inversion is performed by using the Particle Swarm Optimization (PSO) technique to minimize the misfit between measured and theoretical HVSR curves, so as to optimize the agreement of the recorded microtremor data with the modeled underground features.

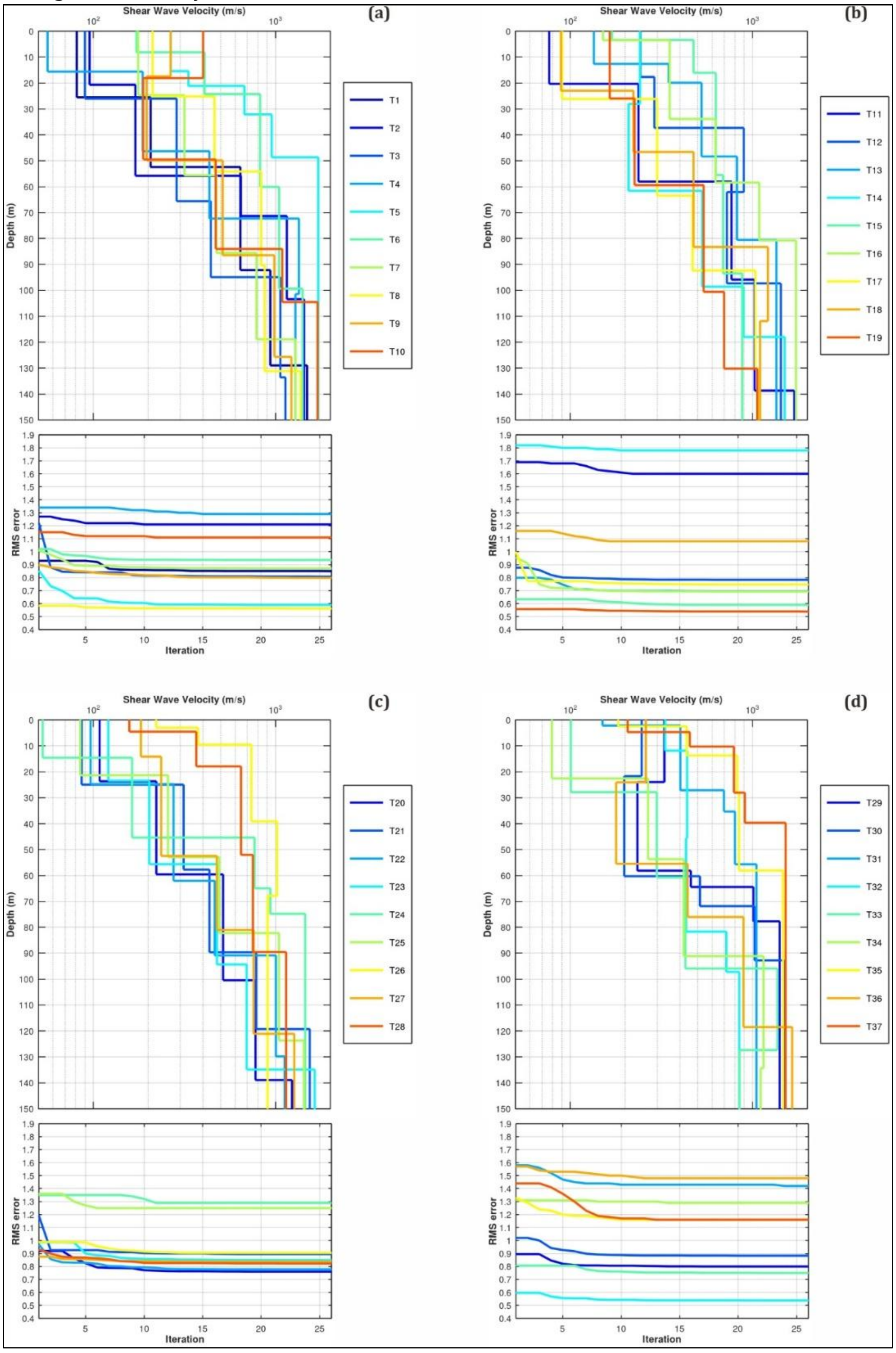

Fig. 5. V_S inversion models from all measurement points, illustrating the variation of subsurface layers across the study area: (a) T1-T10, (b) T11-T19, (c) T20-T28, and (d) T29-T37.

The V_S values derived from modeling results show a significant range, from 52.8 m/s to 1,732.3 m/s. General trends of the V_S values increase as a function of depth in accordance with the overall expected increasing material density and stiffness at greater depths within its subsurface structure. This relationship depicts progradation from loose surface conditions to denser lieinage at depth.

According to the inverted results, the maximum thickness of subsurface layers that could be modelled is over 150 m, ensuring a full coverage of the subsurface structure in our study area. For which is the mean S-wave velocity to a depth of 30m, V_S^{30} values were derived from the first three layers of the model. Together, these layers are approximately 30 m deep and conform to the typical depth that is used to classify sites for seismic purposes.

As summarized in Fig. 5, the low error values (0.5–1.8) from the inversion demonstrate that the model can represent well with the actual subsurface environment. The asymptotic decrease of error from the first to the last iteration indicates that the PSO inversion algorithm is stable and convergent, and can accurately retrieve salient features from the measured HVSR spectra. This indicates that the modelled layer boundaries and V_S^{30} contrasts are geologically plausible for the Kedamaian area.

The inverse-derived S-wave velocity model, in general, is crucially important to describe the subsurface characteristics of the Kedamaian area.

2.5 V_S^{30} Distribution

Fig. 6 maps the shear-wave velocity over the study area, which represents the average stiffness distribution from close to 30 m depth. The V_S^{30} is directly related to ground stiffness: higher values are for dense materials (soil or rock) and compact states; lower values are for soft sediments. Hard soil conditions and relatively high natural frequencies correspond to thin transient sediment layers and small seismic wave amplitudes. In dense or consolidated rocks, elastic waves travel faster and are dissipated through attenuation more effectively, leading to high seismic energy loss during the ground motion and a low seismic hazard. On the other hand, soft soils (i.e., those with thick unconsolidated layers of sediment) can retard wave transmission and consequently may attenuate high-frequency waves to a greater extent than low-frequency ones. The consequence is to concentrate more seismic energy on the surface, which can result in ground acceleration amplification and therefore potential damage of buildings.

From Table 9, the categorization and spatial distribution of V_S^{30} values, which represent the Kedamaian District soil type, measured in this study, can provide information from type C to E for the inclusion of hard, medium, and soft soils. Most of the region, especially over the northern and central parts of the study area, with high depth-averaged shear wave velocity (V_S^{30}) values between 80.9 and 132.6 m/s, associated with unconsolidated tuffaceous and volcanic deposits. The medium soils (type D) are limited to some areas of the central, northeastern, and southeastern regions with velocities ranging from 175 m/s to 350 m/s (191.3-340.0 m/s measured values). Types C soils–hard soils with 357.6 to 511.3 m/s- are distributed in the east and southwest, which represents compact lithology or shallow bedrock exposure.

Geologically, the Lampung Formation (type E), which is dominated by weak volcanic tuff, tuffaceous clay, and a sandy layer as a source of moderate amplification, belongs to the soil type of uniform soft. The Tarahan Formation, on the other hand, mainly consists of type C soils consistent with its lithological character, made by consolidated sedimentary and volcanic materials that decrease the ground shaking level. The Quaternary Volcanic Deposits show a wide span due to their thick heterolithology relationship and the variation in their tectonic structure resulting from complex depositional and volcanic processes.

These results are in agreement with those obtained from the amplifications and dominant frequency analyses, where the sites exhibiting lower V_S^{30} values match well with high A_0 value and low f_0 value, indicating the presence of thick unconsolidated sediments capable of strongly amplifying seismic waves (Harlianto et al., 2025; Qadri et al., 2023). On the contrary, higher V_S^{30} values are associated with lower seismic vulnerability: in this case, ground conditions are more stable and more favorable for infrastructure (Harlianto et al., 2025; Qadri et al., 2023). In general, the distribution map of V_S^{30} can be regarded as an indicative map for understanding the features of the subsurface structure and mechanical properties in the Kedamaian District.

Table 9. Classification of V_S^{30} values.

Point	Type	Soil type
T1-T4, T11, T17-T25, T33-T34	E	Soft soil
T5-T10, T12-T14, T16, T27, T29-T30, T36	D	Medium soil
T15, T26, T28, T31-T32, T35, T37	C	Hard oil

A_0 mapping is still of paramount importance for assessing seismic hazard; in particular, in cities with heterogeneous site response. High amplification conditions in the planning and design of earthquake-resistant constructions should be considered to provide development infrastructure consistent with the nature of site geotechnical properties, which helps reduce effects that could result from earthquakes. Also, the mapping of dominant frequency (f_0) provides a geological understanding of the subsurface and useful input for microzonation, seismic hazard assessment, and earthquake-resistant design in general urban development planning. These studies have suggested that various site responses (A_0, f_0, and K_g) are associated with different subsurface conditions controlling the magnitude of ground motion amplification. Railway-induced change in the four parameters, including V_S^{30}, K_g, A_0, and f_0 can be involved for an assessment of local site effects, which are important in earthquake engineering design, sustainable land use planning, and disaster prevention consultancy. The results of this research will be beneficial for establishing a local seismic microzonation model and will become the scientific basis supporting the efforts toward more resilient and safer land usage in the Bandar Lampung Municipality area.

To improve the reliability and applicability of these results, it is suggested that combining HVSR data with other geophysical methods (e.g., MASW, ReMi, or borehole logging) in future research would provide better constraints on sediment thickness and lithological variations. Regions with high amplification, low dominant frequency, and small V_S^{30} values are suggested for detailed seismic hazard assessment and site-specific response examination. Increasing the number of microtremor measurements would further improve the spatial resolution of microzonation maps for the Kedamaian and its vicinity. These methods, when combined, allow better estimation of the site effects and contribute as a base for well-founded in seismic-resistant buildings construction and urban development planning to encourage Bandar Lampung City.

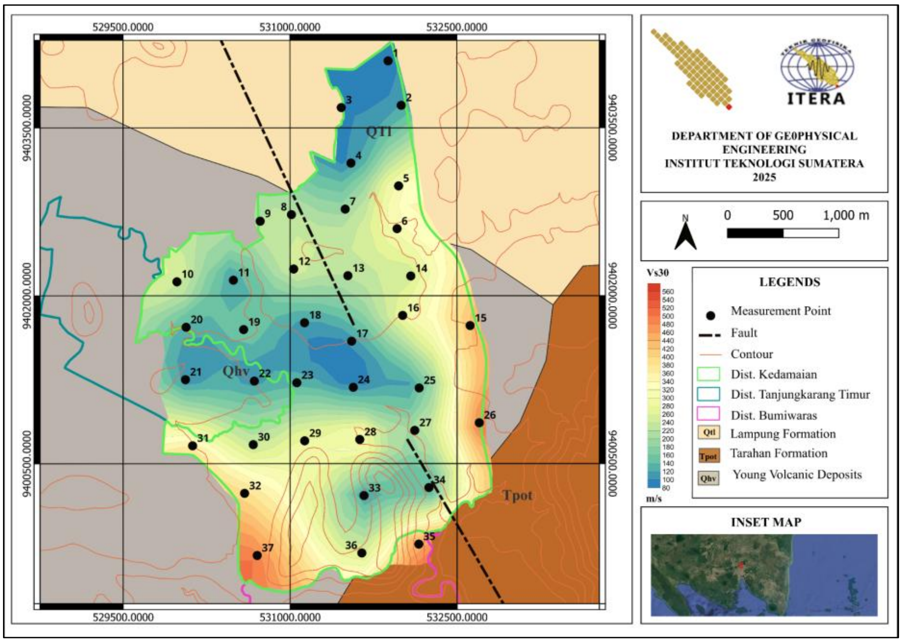

Fig. 6. V_S^{30} distribution map of the study area with superimposed geological formations.

4. Conclusion

The investigation carried out in the Kedamaian District shows that the shallow subsurface consists of thick deposits of sediment having different lithological properties. Amplification (A_0) of seismic waves varies from 2.31 to 9.11, with the majority of localities characterized as moderate. This suggests that the level of ground motion amplification is in general moderate and occasionally strong at some zones. The dominant frequency (f_0) ranges from 0.64 to 18.76 Hz; lower frequencies are associated with thick and soft sediments, whereas higher frequencies represent compacted or dense formations. The K_g is between 0.48 and 119.24, which shows strong spatial variation, and there are regions with high vulnerability caused by both high amplification and low dominant frequency.

The results of the inversion of shear-wave velocity (V_S) indicated that it gradually increases with increasing depth, and the average depths to the interface (V_S^{30}) were in the range from 80.9 m/s to 511.3 m/s; therefore, soft soil types (E) are present over most areas of the study area, followed by soil type D and then soil type C. The dominance of soft deposits in the ground suggests that a significant part of Kedamaian is more susceptible to hard ground shaking during seismic activities, so this category can be classified as moderate to high prone area.

The combination of parameters derived from microtremors (A_0, f_0, K_g, and V_S^{30}) can provide a clear snapshot of local site conditions. These results provide important information for seismic microzonation, earthquake-resistant structural design, and disaster prevention planning. The findings contribute to provide scientific grounds that can be used to sustainable urban practices on disaster and earthquake risk reduction in the Kedamaian District, Bandar Lampung City.

Acknowledgements

The authors would like to express sincere gratitude to the Geophysical Exploration Laboratory for providing access to the Raspberry Shake equipment and to the students of the Geophysical Engineering Study Program at ITERA for their assistance in field data acquisition. Special thanks are also extended to Mr. Alhada Farduwin for granting permission to use the HVSR inversion modeling software.

References

Ahadi, R.W., Ghifari, S. Al, Taufiquds, K.B., Rasyid, M.F. Al, Makki, M.A., Mulyasari, R., 2023. Studi Pendahuluan Potensi Likuefaksi Menggunakan Pendekatan Geologi, Hidrogeologi, dan Data Vs30 pada Kecamatan Kalianda, Lampung Selatan. Journal Online of Physics 8, 70–74. https://doi.org/10.22437/jop.v8i3.27351

Amirudin, Madrinovella, I., Sofian, 2023. Seismic Vulnerability Analysis Using the Horizontal to Vertical Spectral Ratio (HVSR) Method on the West Palu Bay Coastline. Journal of Geoscience, Engineering, Environment, and Technology 8, 23–34. https://doi.org/10.25299/jgeet.2023.8.02-2.13879

Antsiferov, A. V., Glukhov, A.A., Kamburova, L.A., 2025. Analysis data of microseismic monitoring of coal–rock mass. Gornyi Zhurnal 35–40. https://doi.org/10.17580/gzh.2025.03.05

Apriana, Y., Refrizon, Farid, M., Onawa, J., Hardianza, M., Setyowati, Y., Verentina, S., 2025. Analysis of Potential New Flood Basin in Ratu Agung Sub-district Using the HVSR Method. Journal of Geoscience, Engineering, Environment, and Technology 10, 356–363. https://doi.org/10.25299/jgeet.2025.10.3.22541

Ariyanto, A., Farduwin, A., Styawan, Y., Putri, I.A., Junian, W.E., Prasetyo, N., Rizki, R., Wulandari, R., 2024. Pemetaan Kerentanan Seismik Melalui Analisis Mikrotremor HVSR di Wilayah Kecamatan Kemiling dan Sekitarnya. JGE (Jurnal Geofisika Eksplorasi) 10, 82–99. https://doi.org/10.23960/jge.v10i2.393

Asnawi, Y., Muksin, U., Tarniati, Y.P., Simanjuntak, A.V.H., Rizal, S., Syukri, M., 2023. Seismic Vulnerability Based on Microtremor Data and HVSR Method in Krueng

Raya, Aceh Besar, in: AIP Conference Proceedings. p. 020008. https://doi.org/10.1063/5.0119573
Dewi, I.K., Resta, I.L., Amin, S.S., Nuklirullah, N., Juventa, J., Situmorang, S., Ramadhani, A.F., 2023. Analisis Kerentanan Tanah Fakultas Sains dan Teknologi Universitas Jambi dengan Menggunakan Data Mikrotremor. Journal Online of Physics 9, 109–115. https://doi.org/10.22437/jop.v9i1.28788
Farduwin, A., Antosia, R.M., Putri, I.A., Santoso, N.A., Irawati, S.M., 2021. Inversi Data Geolistrik Menggunakan Particle Swarm Optimization: Studi Kasus Desa Gayau. JGE (Jurnal Geofisika Eksplorasi) 7, 88–99. https://doi.org/10.23960/jge.v7i2.118
Farduwin, A., Yudistira, T., 2021. Shear velocity inversion from ambient seismic noise using RR-PSO: A case study of Nusa Tenggara Island, in: Journal of Physics: Conference Series. p. 012022. https://doi.org/10.1088/1742-6596/1949/1/012022
Harlianto, B., Fadli, D.I., Sumanjaya, E., Hadi, A.I., Maulidiyah, A., Suwarsono, Purwanto, E.H., 2025. Seismic Vulnerability Along the Kaur-South OKU Highway in Bengkulu, Indonesia: Planning for More Resilient and Safer Cities. Indian Geotechnical Journal 55, 3042–3057. https://doi.org/10.1007/s40098-024-01101-6
Işık, E., Avcil, F., Büyüksaraç, A., Arkan, E., Harirchian, E., 2025. Impact of Local Soil Conditions on the Seismic Performance of Reinforced Concrete Structures: In the Context of the 2023 Kahramanmaraş Earthquakes. Applied Sciences (Switzerland) 15, 2389. https://doi.org/10.3390/app15052389
Khayati, N.N., Sudarmaji, Hartantyo, E., 2022. The Effect of Weathered Layer Thickness and Slope on Potential Areas of Landslides in Gerbosari Village, Samigaluh District, Kulonprogo Regency, Indonesia. Journal of Geoscience, Engineering, Environment, and Technology 7, 124–131. https://doi.org/10.25299/jgeet.2022.7.3.9161
Kubicek, J., Varysova, A., Cerny, M., Skandera, J., Oczka, D., Augustynek, M., Penhaker, M., 2023. Novel Hybrid Optimized Clustering Schemes with Genetic Algorithm and PSO for Segmentation and Classification of Articular Cartilage Loss from MR Images. Mathematics 11, 1027. https://doi.org/10.3390/math11041027
Künzel, L.A., Leibfarth, S., Dohm, O.S., Müller, A.C., Zips, D., Thorwarth, D., 2020. Automatic VMAT planning for post-operative prostate cancer cases using particle swarm optimization: A proof of concept study. Physica Medica 69, 101–109. https://doi.org/10.1016/j.ejmp.2019.12.007
Ma, H., Liao, B.Y., 2024. Study on Site Effect in Nanning City Using HVSR Method. Civil Engineering and Architecture 12, 1165–1179. https://doi.org/10.13189/cea.2024.120235
Mahapatra, A.K., Panda, N., Pattanayak, B.K., 2023. Hybrid PSO (SGPSO) with the Incorporation of Discretization Operator for Training RBF Neural Network and Optimal Feature Selection. Arabian Journal for Science and Engineering 48, 9991–10019. https://doi.org/10.1007/s13369-022-07408-x
Manan, A., Puspitafuri, C., Chahyani, R., Irawati, Pertiwi, I.I., 2023. Identification of Shear Strain on the Surface Ground of Wangi-Wangi Island, Southeast Sulawesi, Indonesia, Using Nakamura's Technique and the Possibility of Its Impacts. Journal of Geoscience, Engineering, Environment, and Technology 8, 275–280. https://doi.org/10.25299/jgeet.2023.8.4.11780
Mangga, S.A., Amirudin, Suwarti, T., Gafoer, S., Sidarto, 2010. Peta Geologi Lembar Tanjungkarang, Sumatera, Edisi Kedua. ed. Pusat Survei Geologi, Bandung.
Molnar, S., Cassidy, J.F., Castellaro, S., Cornou, C., Crow, H., Hunter, J.A., Matsushima, S., Sánchez-Sesma, F.J., Yong, A., 2018. Application of Microtremor Horizontal-to-Vertical Spectral Ratio (MHVSR) Analysis for Site Characterization: State of the Art. Surveys in Geophysics 39, 613–631. https://doi.org/10.1007/s10712-018-9464-4
Nakamura, Y., 2019. What is the Nakamura method? Seismological Research Letters 90, 1437–1443. https://doi.org/10.1785/0220180376
Nasrudin, A., Sari, A.P., Desmarini, A., Fuadina, F.N., Putri, W.A., 2024. Statistik Daerah Kota Bandar Lampung 2024. Bandar Lampung.
Nateqi, M.H., Amelsakhi, M., Nateqi, M., 2025. A study of the effects of different layering characteristics on the response of two and three-layered semi-sine hills. Iranian Journal of Geophysics 19, 101–120.
Prasetya, A.R., Faris, F., Rahardjo, A.P., 2024. Seismic Vulnerability Assessment Using the HVSR Method at Yogyakarta International Airport Underpass, Indonesia. International Journal of GEOMATE 26, 25–33. https://doi.org/10.21660/2024.114.4082
Qadri, S.M.T., Mirza, M.Q., Raja, A., Yaghmaei-Sabegh, S., Hakimi, M.H., Ali, S.H., Khan, M.Y., 2023. Application of Probabilistic Seismic Hazard Assessment to Understand the Earthquake Hazard in Attock City, Pakistan: A Step towards Linking Hazards and Sustainability. Sustainability 15, 1023. https://doi.org/10.3390/su15021023
Risa, I.N., Maison, M., Dewi, I.K., 2023. Analisis Kerentanan Tanah Berdasarkan Pengukuran Mikrotremor di Desa Jati Mulyo, Tanjung Jabung Timur. JGE (Jurnal Geofisika Eksplorasi) 9, 18–31. https://doi.org/10.23960/jge.v9i1.236
Saadalla, H., Abdelhafiez, H.E., Ali, S., 2023. Seismic station sites response as a discriminant tool between earthquakes and quarry blasts in Aswan region, Upper Egypt. Journal of African Earth Sciences 199, 104826. https://doi.org/10.1016/j.jafrearsci.2022.104826
Simanjuntak, N.S., Umar Muksin, Idris, Y., Andi A. Rusdin, 2025. Resonance and Damping Ratio Analysis of the Baiturrahman Mosque Tower Based on Earthquake Ground Shaking. Journal of Geoscience, Engineering, Environment, and Technology 10, 270–274. https://doi.org/10.25299/jgeet.2025.10.02.21982
Wang, Q., Li, Y., Wu, Y., 2024. Sedimentary structures beneath the Northern Bohai basin constrained by the autocorrelation of receiver function. Chinese Journal of Geophysics (in Chinese) 67, 2291–2303.
Wibowo, N.B., Fathani, T.F., Pramumijoyo, S., Marliyani, G.I., 2024. Comparison of the VS30 model and site class based on MASW, microtremor and N-SPT data in the Opak River Basin, in: IOP Conference Series: Earth and Environmental Science. p. 012002. https://doi.org/10.1088/1755-1315/1373/1/012002
Xv, X., Li, Q., 2023. A Study of Soil Shear Strength Sensing Based on Soil Shear Save Velocity, in: 2023 China Automation Congress (CAC). IEEE, pp. 6382–6387. https://doi.org/10.1109/CAC59555.2023.10451797

Yao, X., Wu, B., 2024. Progress in Seismic Isolation Technology Research in Soft Soil Sites: A Review. Buildings 14, 3198. https://doi.org/10.3390/buildings14103198

Yatini, Y., Kustanto Putra, A., Paripurno, E.T., 2023. Application of HVSR Method on Microtremor Data for Analysis of Earthquake Potential in Candipuro District, Lumajang, Indonesia. Journal of Geoscience, Engineering, Environment, and Technology 8, 288–294. https://doi.org/10.25299/jgeet.2023.8.4.13460

Yudha, A., Laby, D.A., Suprayitno, A., 2023. Implementasi Algoritma Particle Swarm Optimization (PSO) pada Inversi Data Resistivitas 1-D untuk Identifikasi Gas Dangkal. Jurnal Geosaintek 9, 96–105. https://doi.org/10.12962/j25023659.v9i2.18513

Zaenudin, A., Darmawan, I.G.B., Farduwin, A., Wibowo, R.C., 2022. Shear wave velocity estimation based on the particle swarm optimization method of HVSR curve inversion in Bakauheni district, Indonesia. Turkish Journal of Earth Sciences 31, 480–493. https://doi.org/10.55730/1300-0985.1815